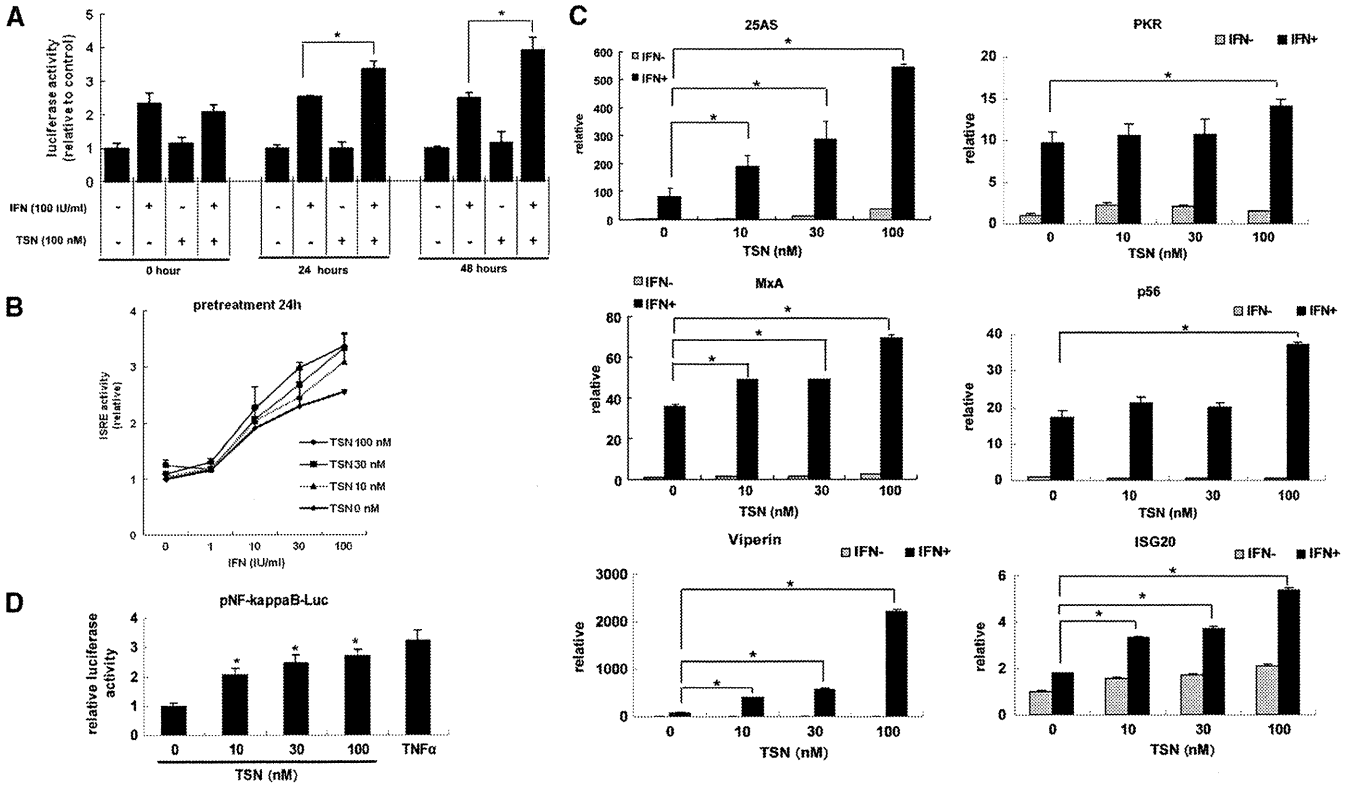

FIG. 3. ISRE reporter screening and aberrant pathway of α-IFN. (A) Pretreatment with TSN. Huh7 cells transfected with a reporter gene (pISRE-Luc and pRL-CMV) were pretreated with TSN (0 or 100 nM) for 0, 24, or 48 h, followed by treatment with α-IFN (0 or 100 IU/ml). Six hours later, the relative ISRE-luciferase activity ($n = 4$) was determined as described in Materials and Methods. The data are expressed as means ± SDs and are a representative example of the data from three similar experiments. (B) Pretreatment with TSN at the concentrations indicated for 24 h, followed by treatment with α-IFN (0 to 100 IU/ml). The ISRE reporter assay was performed as described for panel A. (C) Type I IFN-induced antiviral ISG expression in Huh7 cells. Huh7 cells were treated with TSN for 24 h, followed by treatment with α-IFN at 100 IU/ml for 24 h. The total cellular RNA was then isolated for real-time RT-PCR analysis of the mRNAs of 25AS, MxA, p56, viperin, and ISG20. Beta-actin was used as a control. The data are expressed as means ± SDs and are a representative example of data from three similar experiments. *, $P < 0.05$. (D) Analysis of aberrant pathways of α-IFN signaling under the influence of TSN. Promoter activities of NF-kappaB were analyzed by luciferase reporter assays. These cells were transfected with pNF-kappaB-TA-Luc, pTA-Luc which lacks the enhancer element and which was used as a negative control, and pRL-CMV to normalize transfection efficiency. At 24 h after transfection with these reporters, treatment with TSN (0, 10, 30, 100 nM) was carried out. After 24 h, the relative levels of induction of NF-kappaB activity for each treatment were calculated. TNF-α (50 ng/ml), which was used as a positive control for NF-kappaB, was added 6 h before analysis. The assays were done in triplicate and repeated three times. Error bars indicate means ± SDs. *, $P < 0.05$.

interferon activation site (GAS), or activator protein 1 (AP1) Fluc plasmids. The reporter activities were measured after culture with or without TSN. As shown in Fig. 3D, there was no significant effect of TSN on GAS or AP1 reporter activities (data not shown). In contrast, NF-kappaB reporter activity was significantly elevated by TSN in a dose-dependent fashion.

Synergistic inhibitory effects of TSN and α-IFN on the replicon. We next assessed the effects of TSN combination with α-IFN on the intracellular replication of the HCV genome. Huh7/Rep-Feo cells were treated with various concentrations of TSN (0, 0.01, and 0.03 μg/ml) and α-IFN (0 to 100 IU/ml). Replication of the HCV replicon was suppressed by pretreatment with TSN, followed by treatment with α-IFN, in a dose-dependent manner (Fig. 4A; see Fig. S1 in the supplemental material). The EC_{50} of α-IFN in the absence of TSN was 7.61 IU/ml, while that after pretreatment with 0.03 μg/ml (41 nM) TSN was 3.16 IU/ml. These results indicated that pretreatment with TSN before α-IFN treatment is more effective in inhibiting HCV replication than treatment with α-IFN alone.

Subsequently, we conducted the following assay to determine whether TSN and α-IFN have a synergistic inhibitory effect on the replicon. The relative dose-inhibition curves of α-IFN were plotted for several concentrations of TSN and α-IFN. The curves shifted to the left with increasing concentrations of TSN (Fig. 4B), demonstrating that HCV replication was considerably reduced by the combination compared with that by either TSN or α-IFN alone. An MTS-based cell viability assay did not show significant cytotoxicity from TSN (Fig. 4C). Western blot analysis and densitometry of each blot showed results essentially identical to those from the luciferase assay (Fig. 4D).

We used isobologram analysis to determine whether the anti-HCV effect of TSN is synergistic with that of α-IFN (27, 37). Huh7/Rep-Feo cells were treated with a combination of α-IFN and TSN at an EC_{50} ratio of 1:0, 2:3, 1:4, or 0:1, and the dose-effect plots were drawn (Fig. 4E). The fractional EC_{50}s for α-IFN and TSN were plotted on the x and y axes, respectively, to generate an isobologram (Fig. 4F). Each plot showing

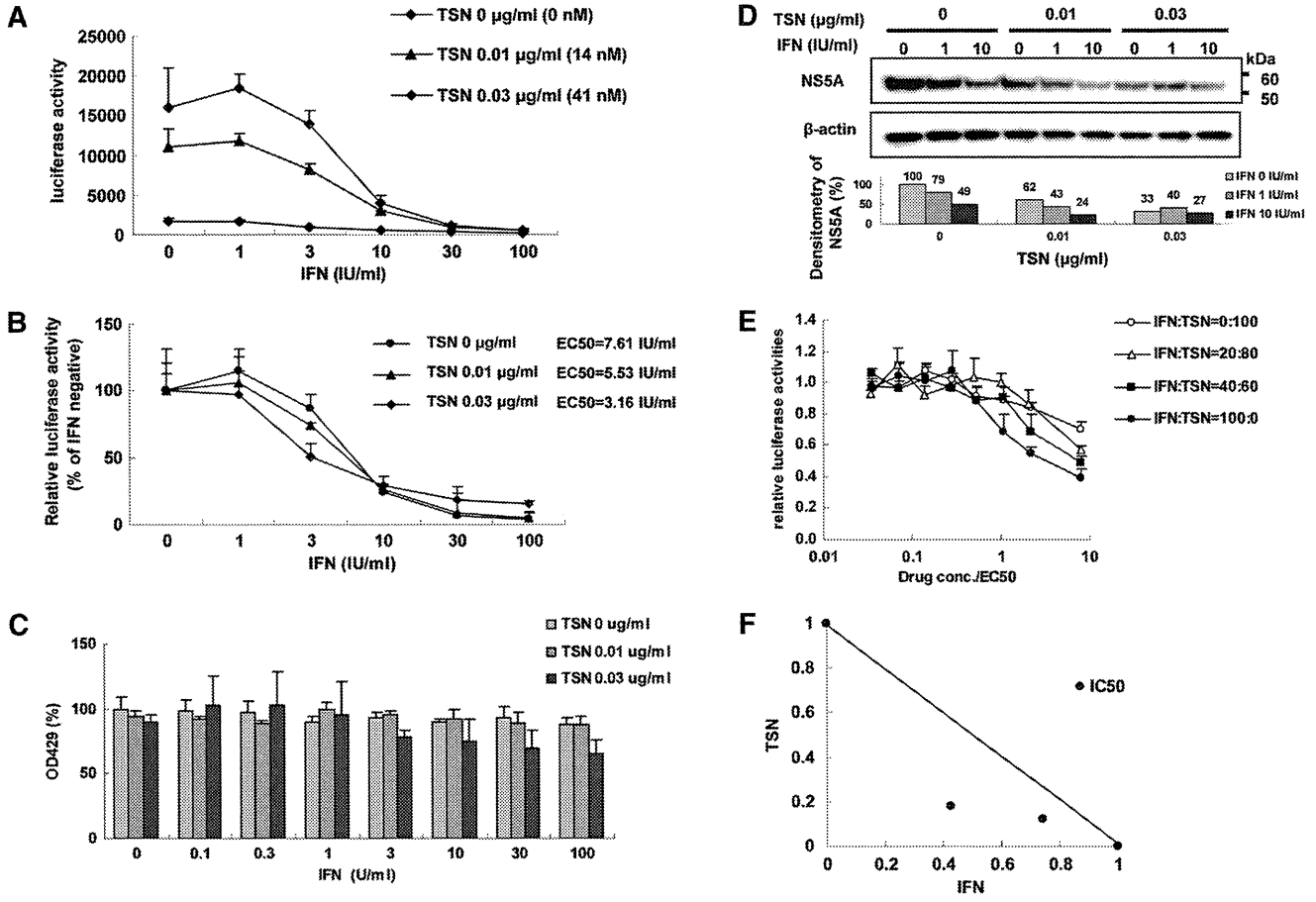

FIG. 4. Suppression of HCV RNA replication by TSN combined with α-IFN. (A and B) Luciferase activity (A, absolute value; B, relative value). Huh7/Rep-Feo cells, which constitutively express an HCV replicon, enable the quantification of replication levels through the measurement of luciferase activity. Absolute and relative dose-response curves in the presence of 24 h of pretreatment of various concentrations of TSN (0, 0.01, 0.03 μg/ml) and α-IFN (0, 100 IU/ml). (A) Bars indicate luciferase activities. (B) Bars indicate luciferase activities relative to the activity of each α-IFN-negative control. Luciferase assays were performed in triplicate. Error bars indicate means ± SDs. (C) MTS assay of Huh7/Rep-Feo cells cultured with the indicated concentrations of TSN and α-IFN. The assays were done in triplicate and repeated three times. Error bars indicate means ± SDs. (D) Western blotting. Ten micrograms of total cellular protein was separated by polyacrylamide gel electrophoresis and transferred onto the membrane. Monoclonal anti-NS5A antibody or an anti-beta-actin antibody was used as the primary antibody. Densitometry of NS5A or beta-actin protein was performed and the result is indicated as a percentage of that for the drug-negative control. The assay was repeated three times, and representative results are shown. (E) Dose-inhibition curves of α-IFN and TSN when they were combined at the indicated ratios, adjusted by the EC_{50} of the individual drug. Assays were done in triplicate, and mean values were plotted and indicated as means ± SDs. (F) Graphical representation of the isobologram analysis. For each drug combination in panel E, the EC_{50}s of α-IFN and TSN for inhibition of HCV replication were plotted against the fractional concentrations of α-IFN and TSN, which are indicated on the *x* and *y* axes, respectively. A theoretical line of additivity is drawn between the EC_{50} for each drug alone. All of the fractional EC_{50} plots for the TSN and α-IFN combinations fell below the line of additivity, indicating synergy.

the fractional EC_{50} of each drug ratio fell below the line showing additivity, indicating that the effect of the drug combination on intracellular HCV RNA replication was synergistic. The MTS values at the drug concentrations used in this isobologram analysis did not show any significant decrease, suggesting that the synergistic action of α-IFN and TSN on HCV replication is through their pharmacological effects and is not due to augmentation of cytotoxicity.

Suppression of HCV-J6/JFH1 infection by pretreatment of TSN with α-IFN. The inhibitory effects of pretreatment with TSN prior to α-IFN treatment demonstrated on HCV subgenomic replication were validated further using HCV-J6/JFH1 cell culture (21, 42). Various concentrations of TSN and α-IFN were added to HCV-J6/JFH1-infected Huh7 cells, and intracellular HCV RNA was quantified after 48 h of incubation. As shown in Fig. 5A, TSN with or without α-IFN suppressed expression of intracellular HCV RNA in a dose-dependent manner. The EC_{50}s of α-IFN with TSN at 0, 10, and 30 nM were 4.71 IU/ml, 3.83 IU/ml, and 3.52 IU/ml, respectively. An MTS-based cell viability assay did not show significant cytotoxicity from TSN (Fig. 5B). These data indicate that pretreatment with TSN also augmented the α-IFN effect on the JFH1 system.

TSN upregulates ISGF3 in combination with α-IFN. Subsequently, we performed experiments to investigate the mechanisms of action of TSN. First, we quantified expression of alpha/beta IFN receptor subunit (IFNAR) 1 and IFNAR2 and the effect of TSN. Real-time RT-PCR analysis showed no

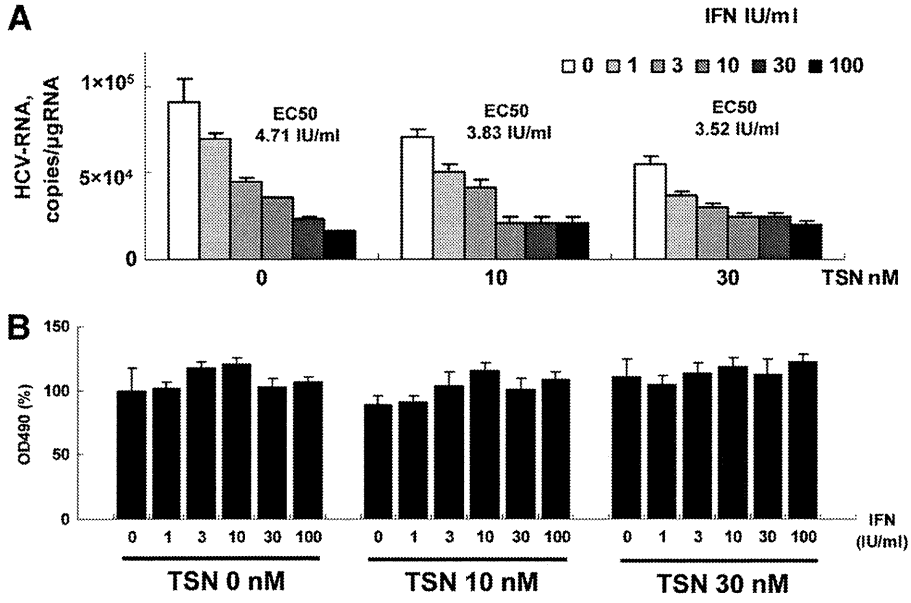

FIG. 5. Suppression of full HCV-J6/JFH1 replication by pretreatment of TSN with α-IFN. Ten micrograms of HCV-J6/JFH1 RNA was transfected into Huh7 cells. At 48 h after transfection, cells were pretreated with TSN for 24 h, followed by treatment with α-IFN (0, 1, 3, 10, 30, 100 IU/ml). At 48 h after α-IFN addition, cells were harvested. (A) Real-time RT-PCR analysis; (B) effect of pretreatment TSN with α-IFN on cell viability. MTS assays were performed 48 h after culture in the presence of pretreatment TSN with α-IFN. Bars indicate values relative to that of the drug-negative control. In panels A and B, the assays were done in triplicate and repeated three times. Error bars indicate means ± SDs.

change in levels of IFNAR1 and IFNAR2 mRNA expression with or without TSN (Fig. 6).

Next, we investigated the ISGF3 components, STAT1, and STAT2, using Western blotting, and interferon regulatory factor 9 (IRF9), using real-time RT-PCR. Huh7 cells were treated with various concentrations of TSN or 0.01% DMSO. Twenty-four hours after TSN treatment, 100 IU/ml of α-IFN was added, and STATs and IRF9 were detected. Western blot analysis demonstrated that phosphorylated STAT1 and STAT2 levels were increased more by treatment with α-IFN and TSN than by α-IFN treatment alone (Fig. 7A and B). In addition, IRF9 mRNA expression was significantly higher following pretreatment with TSN prior to α-IFN therapy than by α-IFN monotherapy (Fig. 8). These findings are consistent with the hypothesis that TSN activates ISGF3 components in combination with α-IFN.

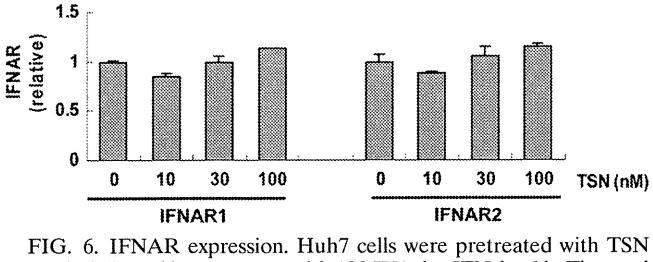

FIG. 6. IFNAR expression. Huh7 cells were pretreated with TSN for 24 h, followed by treatment with 100 IU/ml α-IFN for 6 h. The total cellular RNA was then isolated for real-time RT-PCR analysis of the mRNAs of IFNAR1 and IFNAR2. The assays were done in triplicate and repeated three times. The data are shown as means ± SDs.

DISCUSSION

In this study, we investigated the molecular actions of TSN on HCV replication and on α-IFN-mediated cellular antiviral responses. Treatment of cells expressing an HCV subgenomic replicon with TSN alone specifically inhibited HCV replication with a selectivity index of more than 146 (Fig. 2). In addition, pretreatment of cells with TSN prior to addition of α-IFN augmented α-IFN receptor-mediated, ISRE-regulated gene expression (Fig. 3). Consistent with these findings, TSN pretreatment significantly enhanced the suppressive effects of α-IFN on the HCV replicon and HCV cell culture (Fig. 4 and 5). Finally, we demonstrated that the α-IFN-enhancing effects of TSN are through increased transcriptional activation of a component of ISGF3 (Fig. 7 and 8). Taken together, out results demonstrate that TSN is potentially an effective antiviral agent when it is used alone and especially when it is used in combination with α-IFN and that screening for such α-IFN-enhancing agents may identify promising antiviral therapeutics. Because TSN treatment alone or simultaneous treatment with TSN and α-IFN did not increase ISRE activity or augment α-IFN-mediated ISRE activation, TSN may affect α-IFN sensitivity by upregulating molecules that affect α-IFN receptor-mediated signaling without activating ISRE signaling directly.

Type I interferon plays a central role in eliminating viruses through its innate antiviral activity or following therapeutic application. Binding of α-IFNs to their receptors activates the Jak-STAT pathway to form a complex with ISGF3, which translocates to the nucleus, binds the ISRE located in the promoter/enhancer region of the ISGs, and activates expression of ISGs (28, 39, 40). In this study, we demonstrated that TSN enhanced α-IFN effects by upregulating ISGF3, which

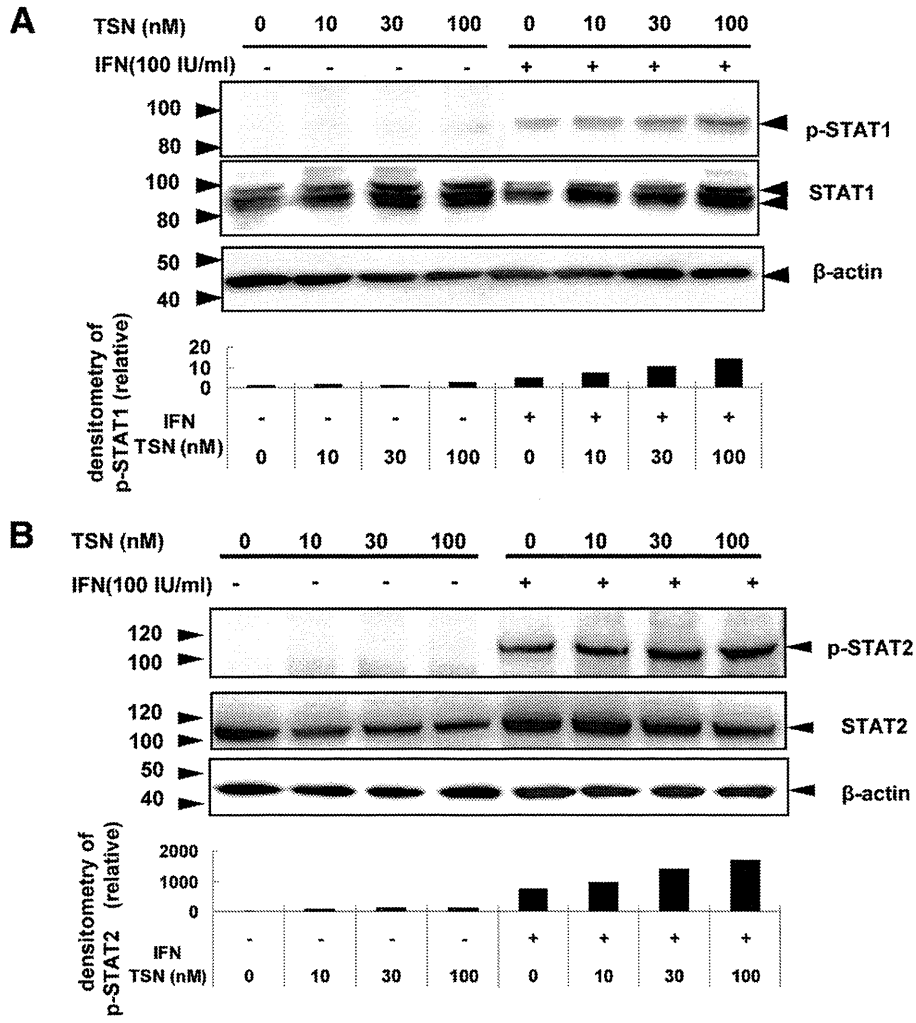

FIG. 7. TSN with α-IFN treatment of Huh7 cells increases phosphorylation of STAT1 and STAT2. (A) Western blotting. Alteration in the distribution of α-IFN-induced phosphorylation of STAT1 and STAT2 by TSN. Huh7 cells were treated with TSN or 0.01% DMSO for 24 h. After that, the cells were stimulated by 100 IU/ml α-IFN for 30 min. Cells were harvested, and the resulting lysates were analyzed for phosphorylated and total STAT1 or STAT2. The relative amounts of phosphorylated STAT1 or STAT2 were normalized to the amount of total STAT1 or STAT2 and expressed relative to the amount for the drug-negative control. The assay was repeated three times, and a representative result is shown.

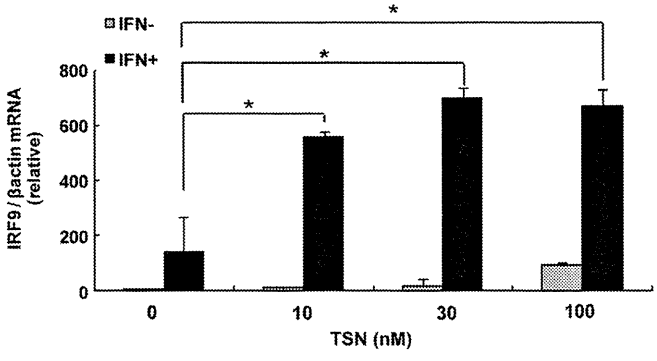

FIG. 8. IRF9 mRNA expression after combination treatment with TSN and α-IFN. Real-time RT-PCR analysis. Huh7 cells were treated with TSN for 24 h. After 6 h, the cells were stimulated by α-IFN (100 IU/ml). We used the method described in the legend to Fig. 6 to analyze the mRNA of IRF9. The assays were done in triplicate and repeated three times. Error bars indicate means ± SDs. *, $P < 0.05$.

may cancel the suppressive effect of HCV gene products on the α-IFN signaling pathway.

In our study, it was not proved that increasing ISRE activities had direct relevance to inhibition of HCV replication. In Fig. 3C, we showed that TSN with α-IFN treatment had elevated the level of expression of mRNA of ISGs. Previous studies suggested that overexpression of known ISGs inhibited HCV replication in HCV replicon-containing Huh7 cells (13, 14). These findings may support the possibility that TSN had the potential to augment the α-IFN effect.

Other than the canonical Jak/STAT-mediated α-IFN signaling pathway, several alternative α-IFN pathways have been reported, including the NF-kappaB, gamma IFN, PI3K, and MAPK pathways (9, 16, 24, 28). We carried out reporter assays using NF-kappaB, AP1, and GAS reporter plasmid constructs and treated the cells with TSN. As shown in Fig. 3D, TSN activated NF-kappaB-regulated gene expression significantly. NF-kappaB is a sequence-specific transcription factor which

regulates the expression of numerous cellular and viral genes and plays important roles in inflammation, innate immune responses, tumorigenesis, and cell survival (3, 19). Activation of NF-kappaB is principally regulated by tumor necrosis factor alpha (TNF-α), Toll-like receptors (TLRs), and RIG-I, which may possibly be associated with the molecular mechanisms of TSN monotherapy. Horsmans et al. (12) and Agrawal and Kandimalla (1) reported that TLR7, -8, and -9 agonists have the ability to modulate TLR-mediated immune responses in targeting a broad range of disease vectors, including HCV, alone or in combination with other therapeutic agents. These reports support the hypothesis that activation of NF-kappaB may be one of the mechanisms of action of TSN.

It has been reported that TSN exhibits cytotoxic/antiproliferative potential at high concentrations (36, 47). In our study, the selectivity index of TSN against HCV was sufficient to ascertain that the antiviral effects are not simply due to the cytotoxicity of TSN. A recent study showed that a triterpenoid compound, dammarenolic acid, inhibits retrovirus, human immunodeficiency virus, simian immunodeficiency virus, murine leukemia virus, and respiratory syncytial virus infections *in vitro* (4) (5). We have analyzed the effects of dammarenolic acid on antiviral actions on Huh7/Rep-Feo cells, cytotoxicity, and ISRE reporter activation. However, dammarenolic acid did not inhibit HCV replication or enhanced α-IFN-induced ISRE activity (data not shown). These findings suggest that the anti-HCV and α-IFN enhancer effects are distinctive features of TSN among triterpenoid compounds. Hiasa et al. have reported that ME3738, a triterpenoid saponin, suppressed HCV replication through production of endogenous beta interferon (11). ME3738 is now in clinical trials for treatment of HCV-infected patients. Taking these findings together, despite reports on the cell-suppressive effect of triterpenoids, properly selected or designed compounds might be used as drugs against HCV infection.

Because the mechanisms of action of these triterpenoid compounds against these viruses are poorly understood, further investigation of the mechanism of action of TSN on HCV may be valuable to implement antiviral strategies against other viruses. It would be important to assess drug resistance after continuous treatment with TSN. There is no *in vitro* or *in vivo* report on resistance of TSN or cellular attenuation of responses to TSN. Such information, if any is found, would help elucidate the mechanism of action of TSN.

Given the current situation of limited therapeutic options against HCV, the search for more potent and less toxic antiviral drugs is needed to improve clinical anti-HCV chemotherapeutics. Several direct antiviral agents with activity against HCV are currently undergoing clinical trials. These include NS3 protease inhibitors and NS5B polymerase inhibitors (41). However, the frequent emergence of drug-resistant viruses is a major weakness of such agents (20). Our results indicate that TSN is also effective at suppressing HCV infection and replication. Future studies with TSN, its derivatives, and other chemicals that target the α-IFN pathway could be directed toward developing a new class of antiviral treatment regimens and drugs.

ACKNOWLEDGMENTS

We thank Frank Chisari for providing Huh7.5.1 cells, Charles Rice for providing plasmid pJ6/JFH1full, and Takaji Wakita for providing plasmid pJFH1full.

This study was supported by grants from the Ministry of Education, Culture, Sports, Science and Technology of Japan, the Japan Society for the Promotion of Science, the Ministry of Health, Labor and Welfare of Japan, the Japan Health Sciences Foundation, the National Institute of Biomedical Innovation, and the Miyakawa Memorial Research Foundation.

REFERENCES

1. **Agrawal, S., and E. R. Kandimalla.** 2007. Synthetic agonists of Toll-like receptors 7, 8 and 9. Biochem. Soc. Trans. **35:**1461–1467.
2. **Bailey, M., N. A. Williams, A. D. Wilson, and C. R. Stokes.** 1992. PROBIT: weighted probit regression analysis for estimation of biological activity. J. Immunol. Methods **153:**261–262.
3. **Baldwin, A. S., Jr.** 2001. Series introduction: the transcription factor NF-kappaB and human disease. J. Clin. Invest. **107:**3–6.
4. **Esimone, C. O., et al.** 2008. Potential anti-respiratory syncytial virus lead compounds from Aglaia species. Pharmazie **63:**768–773.
5. **Esimone, C. O., et al.** Dammarenolic acid, a secodammarane triterpenoid from Aglaia sp. shows potent anti-retroviral activity in vitro. Phytomedicine **17:**540-547.
6. **Fried, M. W., et al.** 2002. Peginterferon alfa-2a plus ribavirin for chronic hepatitis C virus infection. N. Engl. J. Med. **347:**975–982.
7. **Funaoka, Y., et al.** Analysis of interferon signaling by infectious hepatitis C virus clones with substitutions of core amino acids 70 and 91. J. Virol., in press.
8. **Ge, D., et al.** 2009. Genetic variation in IL28B predicts hepatitis C treatment-induced viral clearance. Nature **461:**399–401.
9. **Goodbourn, S., L. Didcock, and R. E. Randall.** 2000. Interferons: cell signalling, immune modulation, antiviral response and virus countermeasures. J. Gen. Virol. **81:**2341–2364.
10. **Hadziyannis, S. J., et al.** 2004. Peginterferon-alpha2a and ribavirin combination therapy in chronic hepatitis C: a randomized study of treatment duration and ribavirin dose. Ann. Intern. Med. **140:**346–355.
11. **Hiasa, Y., et al.** 2008. Hepatitis C virus replication is inhibited by 22beta-methoxyolean-12-ene-3beta, 24(4beta)-diol (ME3738) through enhancing interferon-beta. Hepatology **48:**59–69.
12. **Horsmans, Y., et al.** 2005. Isatoribine, an agonist of TLR7, reduces plasma virus concentration in chronic hepatitis C infection. Hepatology **42:**724–731.
13. **Itsui, Y., et al.** 2009. Antiviral effects of the interferon-induced protein guanylate binding protein 1 and its interaction with the hepatitis C virus NS5B protein. Hepatology **50:**1727–1737.
14. **Itsui, Y., et al.** 2006. Expressional screening of interferon-stimulated genes for antiviral activity against hepatitis C virus replication. J. Viral Hepat. **13:**690–700.
15. **Jiang, D., et al.** 2008. Identification of three interferon-inducible cellular enzymes that inhibit the replication of hepatitis C virus. J. Virol. **82:**1665–1678.
16. **Kalvakolanu, D. V.** 2003. Alternate interferon signaling pathways. Pharmacol. Ther. **100:**1–29.
17. **Kanazawa, N., et al.** 2004. Regulation of hepatitis C virus replication by interferon regulatory factor 1. J. Virol. **78:**9713–9720.
18. **Karakama, Y., et al.** 2010. Inhibition of hepatitis C virus replication by a specific inhibitor of serine-arginine-rich protein kinase. Antimicrob. Agents Chemother. **54:**3179–3186.
19. **Karin, M., and A. Lin.** 2002. NF-kappaB at the crossroads of life and death. Nat. Immunol. **3:**221–227.
20. **Kuntzen, T., et al.** 2008. Naturally occurring dominant resistance mutations to hepatitis C virus protease and polymerase inhibitors in treatment-naive patients. Hepatology **48:**1769–1778.
21. **Lindenbach, B. D., et al.** 2005. Complete replication of hepatitis C virus in cell culture. Science **309:**623–626.
22. **Mishima, K., et al.** 2010. Cell culture and in vivo analyses of cytopathic hepatitis C virus mutants. Virology **405:**361–369.
23. **Nakagawa, M., et al.** 2005. Suppression of hepatitis C virus replication by cyclosporin a is mediated by blockade of cyclophilins. Gastroenterology **129:**1031–1041.
24. **Randall, R. E., and S. Goodbourn.** 2008. Interferons and viruses: an interplay between induction, signalling, antiviral responses and virus countermeasures. J. Gen. Virol. **89:**1–47.
25. **Sadler, A. J., and B. R. Williams.** 2008. Interferon-inducible antiviral effectors. Nat. Rev. Immunol. **8:**559–568.
26. **Sakamoto, N., and M. Watanabe.** 2009. New therapeutic approaches to hepatitis C virus. J. Gastroenterol. **44:**643–649.
27. **Sakamoto, N., et al.** 2007. Bone morphogenetic protein-7 and interferon-alpha synergistically suppress hepatitis C virus replicon. Biochem. Biophys. Res. Commun. **357:**467–473.

28. **Samuel, C.** 2001. Antiviral actions of interferons. Clin. Microbiol. Rev. **14:**778–809.
29. **Sangiovanni, A., et al.** 2006. The natural history of compensated cirrhosis due to hepatitis C virus: a 17-year cohort study of 214 patients. Hepatology **43:**1303–1310.
30. **Sekine-Osajima, Y., et al.** 2008. Development of plaque assays for hepatitis C virus-JFH1 strain and isolation of mutants with enhanced cytopathogenicity and replication capacity. Virology **371:**71–85.
31. **Shi, Y. L., and M. F. Li.** 2007. Biological effects of toosendanin, a triterpenoid extracted from Chinese traditional medicine. Prog. Neurobiol. **82:**1–10.
32. **Shi, Y. L., and Z. F. Wang.** 2004. Cure of experimental botulism and antibotulismic effect of toosendanin. Acta Pharmacol. Sin. **25:**839–848.
33. **Soothill, J. S., R. Ward, and A. J. Girling.** 1992. The IC50: an exactly defined measure of antibiotic sensitivity. J. Antimicrob. Chemother. **29:**137–139.
34. **Suda, G., et al.** IL-6-mediated intersubgenotypic variation of interferon sensitivity in hepatitis C virus genotype 2a/2b chimeric clones. Virology **407:**80–90.
35. **Suppiah, V., et al.** 2009. IL28B is associated with response to chronic hepatitis C interferon-alpha and ribavirin therapy. Nat. Genet. **41:**1100–1104.
36. **Tada, K., M. Takido, and S. Kitanaka.** 1999. Limonoids from fruit of Melia toosendan and their cytotoxic activity. Phytochemistry **51:**787–791.
37. **Tanabe, Y., et al.** 2004. Synergistic inhibition of intracellular hepatitis C virus replication by combination of ribavirin and interferon-alpha. J. Infect. Dis. **189:**1129–1139.
38. **Tanaka, Y., N. Nishida, M. Sugiyama, K. Tokunaga, and M. Mizokami.** Lambda-interferons and the single nucleotide polymorphisms: a milestone to tailor-made therapy for chronic hepatitis C. Hepatol. Res. **40:**449–460.
39. **Taniguchi, T., K. Ogasawara, A. Takaoka, and N. Tanaka.** 2001. IRF family of transcription factors as regulators of host defense. Annu. Rev. Immunol. **19:**623–655.
40. **Taniguchi, T., and A. Takaoka.** 2002. The interferon-alpha/beta system in antiviral responses: a multimodal machinery of gene regulation by the IRF family of transcription factors. Curr. Opin. Immunol. **14:**111–116.
41. **Thompson, A. J., and J. G. McHutchison.** 2009. Antiviral resistance and specifically targeted therapy for HCV (STAT-C). J. Viral Hepat. **16:**377–387.
42. **Wakita, T., et al.** 2005. Production of infectious hepatitis C virus in tissue culture from a cloned viral genome. Nat. Med. **11:**791–796.
43. **Yokota, T., et al.** 2003. Inhibition of intracellular hepatitis C virus replication by synthetic and vector-derived small interfering RNAs. EMBO Rep. **4:**602–608.
44. **Zeuzem, S., et al.** 2000. Peginterferon alfa-2a in patients with chronic hepatitis C. N. Engl. J. Med. **343:**1666–1672.
45. **Zhang, B., Z. F. Wang, M. Z. Tang, and Y. L. Shi.** 2005. Growth inhibition and apoptosis-induced effect on human cancer cells of toosendanin, a triterpenoid derivative from Chinese traditional medicine. Invest. New Drugs **23:**547–553.
46. **Zhang, J. H., T. D. Chung, and K. R. Oldenburg.** 1999. A simple statistical parameter for use in evaluation and validation of high throughput screening assays. J. Biomol. Screen. **4:**67–73.
47. **Zhang, Y., et al.** 2008. Roles of reactive oxygen species and MAP kinases in the primary rat hepatocytes death induced by toosendanin. Toxicology **249:** 62–68.
48. **Zhong, J., et al.** 2005. Robust hepatitis C virus infection in vitro. Proc. Natl. Acad. Sci. U. S. A. **102:**9294–9299.

Hepatology Research

Hepatology Research 2011; **41**: 258–269 doi: 10.1111/j.1872-034X.2010.00771.x

Original Article

Studies on virus kinetics using infectious fluorescence-tagged hepatitis C virus cell culture

Machi Yamamoto,[1]* Naoya Sakamoto,[1,2]* Tetsuya Nakamura,[1,3] Yasuhiro Itsui,[1,5] Mina Nakagawa,[1,2] Yuki Nishimura-Sakurai,[1] Sei Kakinuma,[1,2] Seishin Azuma,[1] Kiichiro Tsuchiya,[1] Takanobu Kato,[4] Takaji Wakita[4] and Mamoru Watanabe[1]

[1]*Department of Gastroenterology and Hepatology,* [2]*Department for Hepatitis Control,* [3]*Department of Advanced Therapeutics in Gastrointestinal Diseases, Tokyo Medical and Dental University,* [4]*Department of Virology II, National Institute of Infectious Disease, Tokyo, and* [5]*Department of Internal Medicine, Soka Municipal Hospital, Saitama, Japan*

Aim: Studies of the complete hepatitis C virus (HCV) life cycle have become possible with the development of a HCV-JFH1 cell culture system.

Methods: In this study, we constructed two fluorescence protein-tagged recombinant JFH1 virus clones, JFH1-EYFP and JFH1-AsRed, as well as two corresponding clones with adaptive mutations, JFH1-EYFP mutant and JFH1-AsRed mutant, that and were as effective as JFH1 in producing infectious virus particles, and investigated their viral infection life cycles.

Results: After infection of the fluorescence-tagged mutant viruses, infected cells increased exponentially. In cells, EYFP or AsRed and NS5A were expressed as a fusion protein and co-localized in core proteins. The rate of the cell–cell spread was dependent on the cell densities with a maximum of $10^{2.5}$/day. Treatment of cells with interferon or a protease inhibitor suppressed expansion of virus-positive cells.

Conclusion: Taken together, these results indicate that fluorescence-tagged HCV is a useful tool to study virus infection life cycles and to assist in the search for novel antiviral compounds.

Key words: AsRed, confocal laser microscopy, HCV-JFH1 cell culture, protease inhibitor, yellow fluorescence protein

INTRODUCTION

HEPATITIS C VIRUS (HCV) infection is characterized frequently by chronic inflammation of the liver, leading to decompensated liver cirrhosis and hepatocellular cancers.[1] Interferon (IFN)-α has been the mainstay of HCV therapy.[2] However, the most effective therapy, pegylated IFN plus ribavirin in combination, can eliminate HCV from only half of the patients treated[3,4] and often is accompanied by substantial side-effects.[5,6] These difficulties in eliminating the virus are attributable mostly to the limited treatment options.[7]

Correspondence: Dr Naoya Sakamoto, Department of Gastroenterology and Hepatology, Tokyo Medical and Dental University, 1-5-45 Yushima, Bunkyo-ku, Tokyo 113-8519, Japan. Email: nsakamoto.gast@tmd.ac.jp

*M. Y. and N. S. contributed equally to this work.

Received 15 July 2010; revised 21 November 2010; accepted 12 December 2010.

Hepatitis C virus belongs to the family Flaviviridae. The viruses have positive-strand RNA genomes of approximately 10 kb that encode polyproteins of approximately 3000 amino acids. The protein is post-translationally processed by cellular and viral proteases into at least 10 mature proteins. The viral non-structural (NS) proteins accumulate in the endoplasmic reticulum (ER) and they direct genomic replication and viral protein synthesis.[8,9] Studies of the HCV life cycle and the development of new drugs have long been hampered by the lack of cell culture systems. These problems have been greatly overcome by the development of the HCV subgenomic replicon[10] and HCV-JFH1 cell culture[11] systems.

After the development of HCV-JFH1 cell culture, many variations of reporter protein-tagged HCV systems have been described.[12–15] These reporter systems, however, feature poor or absent virus propagation, secretion and re-infection. The C-terminal end of the NS5A region, which has been used for insertion of

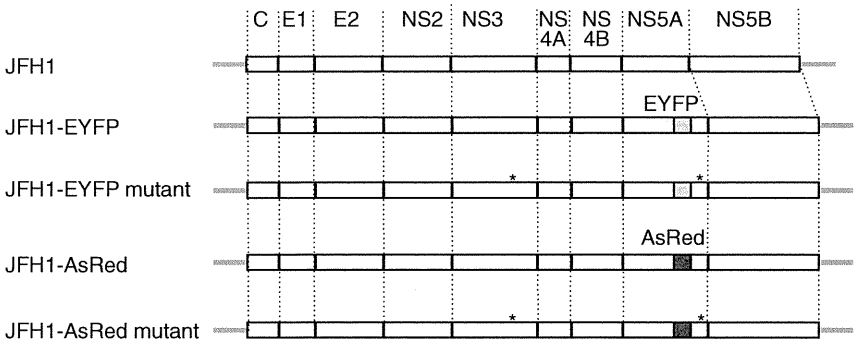

Figure 1 Schematic of the JFH1-based hepatitis C virus constructs. EYFP or AsRed was inserted in-frame into the *Cpo*I site of NS5A (JFH1-EYFP or JFH1-AsRed). The adaptive mutations in NS3 and NS5A (T4209A and C7653T) are indicated by asterisks (JFH1-EYFP mutant or JFH1-AsRed mutant).

reporter sequences, does not affect viral genomic replication,[12] while manipulation of the domain resulted in the loss of viral particle secretion possibly through abrogation of NS5A-core protein–protein association that is crucial for the viral particle assembly.[16] These problems have made it to difficult to analyze the entire viral life cycle in living cells. Recently, Han *et al.* reported a mutant HCV-JFH1 clone that expressed green fluorescent protein (GFP)-tagged NS5A and which could propagate and secrete infectious virus particles.[17]

In this study, we took advantage of the mutant fluorescence protein-tagged HCV and investigated the life cycles of HCV infection. We have demonstrated the rate of expansion of HCV infection using flow cytometry. Moreover, we have shown the kinetics of co-infection with two virus strains, which differed in their ability to secrete infectious virus particles.

METHODS

Reagents

RECOMBINANT HUMAN IFN-α-2b was from Schering-Plough (Kenilworth, NJ). Protease inhibitor (BILN2061) was from Boehringer Ingelheim (Ingelheim, Germany). BILN2061 is a macrocyclic NS3 protease inhibitor, the antiviral effects of which have been reported in a phase I clinical study.[18] Although further development of BILN2061 has been abandoned, this compound has structural homology with other protease inhibitors that are currently being evaluated in clinical trials, such as TMC435 and MK7009.[7,19]

Cell culture

Huh7.5.1 cells[20] and their derivatives were maintained in Dulbecco's modified minimal essential medium (DMEM; Sigma, St Louis, MO, USA) with 10% fetal bovine serum (FBS; Invitrogen, San Diego, CA, USA) at 37°C under 5% CO_2.

Plasmid constructs (Fig. 1)

In order to produce pJFH1-EYFP, the EYFP gene was amplified from pEYFP-C1 (Clontech, Mountain View, CA, USA) by polymerase chain reaction (PCR). The PCR products were then inserted into the *Cpo*I site (7484) of pJFH1. Similarly, pJFH1-AsRed was produced using pAsRed2 (Clontech). The JFH1-EYFP and JFH1-AsRed mutants, which are JFH1-based mutants with robust virus production capability, have two point mutations (T4209A, C7653T).[17] In order to introduce these mutations into pJFH1-AsRed, the *Avr*II/*Nsi*I and *Bsr*GI fragments of pJFH1-AsRed were amplified by PCR. The PCR products were subcloned into the T-Vector (pGEM-T Easy Vector Systems; Promega, Madison, WI, USA) and the mutations were introduced by site-directed mutagenesis (Quick-Change II Site-Directed Mutagenesis Kit; Stratagene, La Jolla, CA, USA), as reported previously.[21] Finally, these *Avr*II/*Nsi*I and *Bsr*GI fragments were reinserted into the parental plasmid, pJFH1-AsRed. The pJFH1-AsRed mutant was digested with *Cpo*I and the DNA fragment was subcloned into pJFH1-EYFP, producing the mutant pJFH1-EYFP. All nucleotide numbers refer to pJFH1.[11]

Constitutive expression of ER-fluorescence protein in Huh7.5.1 cells

Huh7.5.1 cells were seeded into 6-cm diameter dishes and transfected with pDsRed2-ER (Invitrogen) using Lipofectamine 2000 (Invitrogen) according to the manufacturer's protocol. Isolated clones (ER-Huh7.5.1 cells) were maintained under selection with 0.75 mg/mL G418 (Nacalai Tesque, Kyoto, Japan) and

screened for DsRed protein expression using fluorescence microscopy (BZ-8000; Keyence, Tokyo, Japan).

RNA transcription and transfection

Recombinant HCV RNA was synthesized and transfected as previously described.[22,23] Briefly, the plasmids were linearized by digestion with *Xba*I and subjected to *in vitro* transcription using RiboMax Large Scale RNA Production System (Promega). For the RNA transfection, Huh7.5.1 cells were suspended in Opti-MEM (Invitrogen) containing 10 μg of HCV RNA, transferred into a 4-mm electroporation cuvette, and subjected to an electric pulse (1050 μF and 270 V) using the Gene Pulser II apparatus (Bio-Rad, Richmond, CA, USA). After electroporation, the cell suspension was left for 5 min at room temperature and then incubated under normal culture conditions in a 10-cm diameter dish. The transfected cells were split every 3–5 days. The culture media were transferred subsequently onto uninfected Huh7.5.1 cells.

Immunofluorescence microscopy

Immunofluorescence microscopy was performed as described previously.[24] Cells were cultured on 18-mm round cover slips (Matsunami, Osaka, Japan) and fixed using 4% paraformaldehyde for 10 min at room temperature. Cells were incubated with the primary antibodies for 1 h at 37°C and with Alexa Fluor 488 goat antimouse immunoglobulin (Ig)G antibody (Molecular Probes, Eugene, OR, USA) for 1 h at room temperature in the dark. Mouse anti-NS5A antibody (Biodesign, Saco, ME, USA) and mouse anti-core antibody (Abcam, Cambridge, MA, USA) were used as primary antibodies. Cells were mounted with VECTA SHIELD Mounting Medium with DAPI (Vector Laboratories, Burlingame, CA, USA) and visualized by confocal laser fluorescent microscopy (BZ-8000 [Keyence] and FLUOVIEW FV10i [Olympus, Tokyo, USA]).[25]

Flow cytometry

JFH1-EYFP and JFH1-EYFP mutant-transfected Huh7.5.1 cells and uninfected Huh7.5.1 cells were cultured in 12-well plates (Becton Dickinson, Franklin Lakes, NJ, USA). The cells were collected on the days, post-transfection or post-infection, indicated. After washing with phosphate buffered saline (PBS; Nacalai Tesque) supplemented with 3% FBS and staining of dead cells with propidium iodide, the cells were analyzed using a FACS Calibur with CellQuest software (Becton Dickinson).

Quantification of HCV core antigen in the culture medium

The culture media from Huh7.5.1 cells transfected with JFH1 and its derivatives were collected on the days indicated and stored at 80°C. The levels of core antigen in the culture media were measured using a chemiluminescence enzyme immunoassay (CLEIA) according to the manufacturer's protocol (Lumipulse Ortho HCV Antigen; Ortho-Clinical Diagnostics).

Western blotting

Western blotting was carried out as described previously.[21] Briefly, 10 μg of total cell lysate was separated by sodium dodecylsulfate polyacrylamide gel electrophoresis and blotted onto a polyvinylidene fluoride membrane. The membrane was incubated with primary antibodies followed by peroxidase-labeled anti-IgG antibody and visualized by chemiluminescence using the ECL Western blotting Analysis System (Amersham Biosciences). The antibodies used were anti-core mouse monoclonal antibody 2H9, anti-NS5A mouse monoclonal antibody 9E10 (provided by Dr Rice), and anti-GFP rabbit polyclonal antibody (Invitrogen). The anti-GFP is able to detect EYFP. To confirm expression of EGFP in Huh 7.5.1 cells, Huh7.5.1 cells were seeded into a 6-cm diameter dish and transfected with pEGFP (Invitrogen) using Lipofectamine 2000 (Invitrogen).

Statistical analyses

Statistical analyses were performed using Welch's *t*-test. *P*-values of less than 0.05 were considered statistically significant.

Figure 2 Infectious hepatitis C virus (HCV) reporter virus with robust virus production capability. (a) Huh7.5.1 cells were transfected with JFH1-EYFP, JFH1-EYFP mutant, JFH1-AsRed or JFH1-AsRed mutant HCV RNA. At 3 days post-transfection, culture media were collected and added onto uninfected cells. At the days indicated, EYFP or AsRed-directed-fluorescence was visualized directly. (b) The ratio of EYFP or AsRed-positive cells in (a) is counted in each image and plotted vs time. Assays were carried out in triplicate and the results are expressed as mean ± standard deviation. $^*P < 0.05$. —●—, JFH1-EYFP mutant; ·○·, JFH1-EYFP; —▲—, JFH1-AsRed mutant; ·△·, JFH1-AsRed. (c) The levels of core antigen in the culture medium of JFH1, JFH1-EYFP, JFH1-EYFP mutant, JFH1-AsRed, and JFH1-AsRed mutant-transfected Huh7.5.1 cells collected on the days indicated. Ag, antigen. ·■·, JFH1; ·○·, JFH1-EYFP; —●—, JFH1-EYFP mutant; ·△·, JFH1-AsRed; —▲—, JFH1-AsRed mutant.

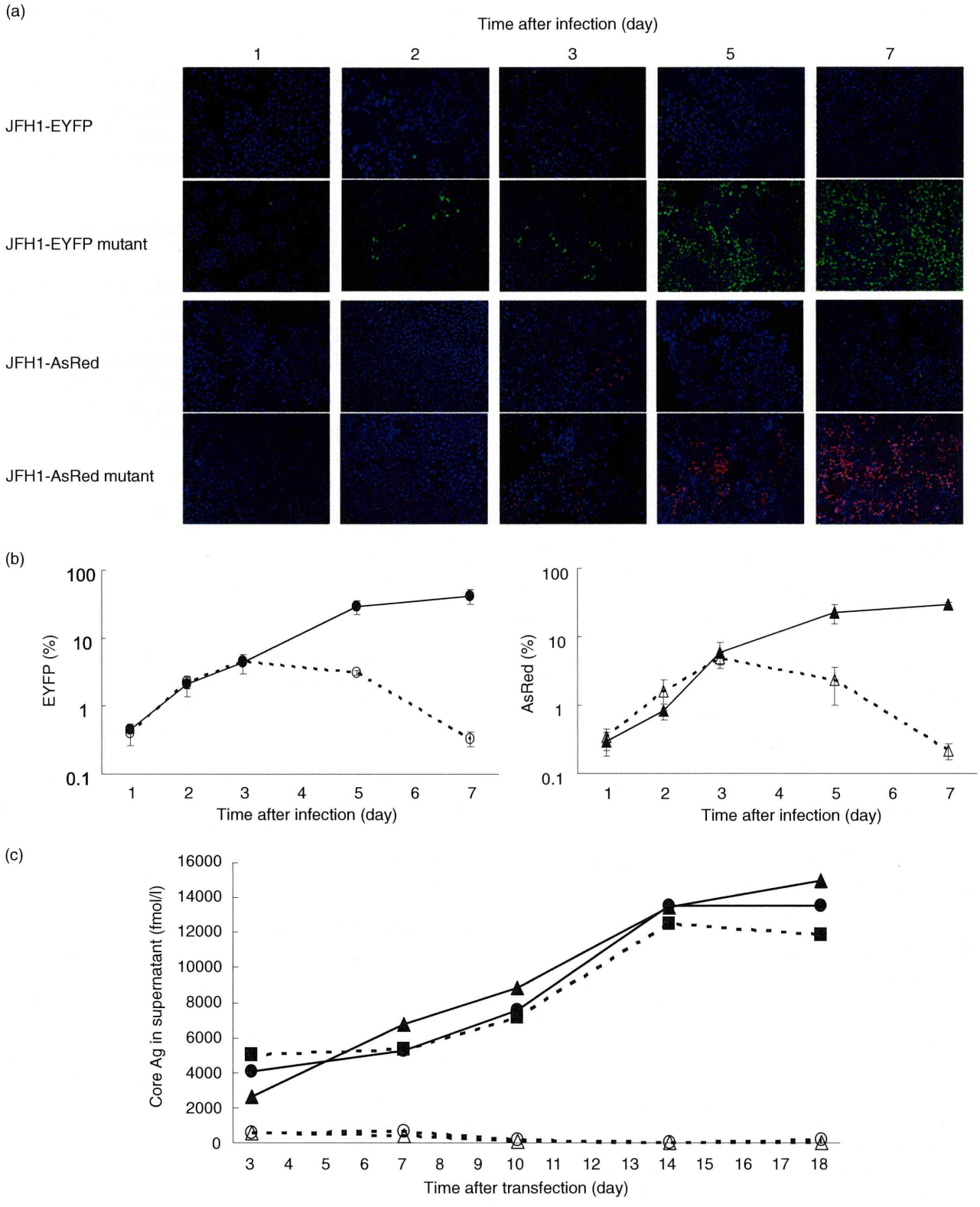

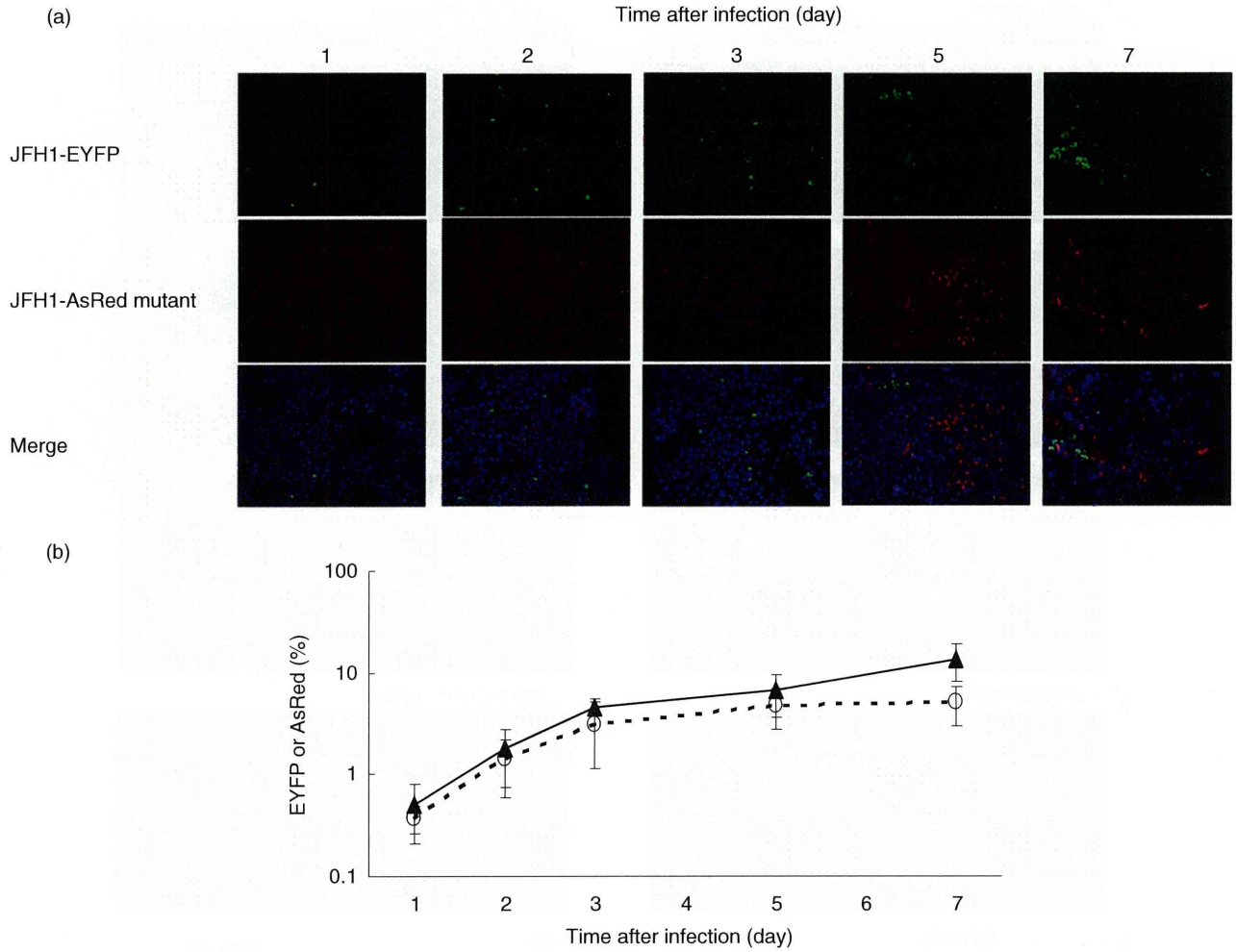

Figure 3 Intracellular *trans*-complementation of virus proteins. (a) Culture media from JFH1-EYFP and JFH1-AsRed mutant-transfected cells at 3 days post-transfection were added onto uninfected Huh7.5.1 cells. At the days indicated, EYFP or AsRed-directed-fluorescence was visualized directly. (b) The ratio of EYFP or AsRed-positive cells in Fig. 2a is calculated and plotted vs time. Assays were carried out in triplicate and the results are expressed as mean ± standard deviation. —▲— JFH1-AsRed mutant; ···◇··· JFH1-EYFP.

RESULTS

Infectious HCV reporter virus with robust virus production capability

FIRST, WE STUDIED whether the JFH1-EYFP mutant viruses are able to secrete sufficient amounts of infectious virus particles. Full-length HCV RNA was transcribed *in vitro* and transfected into Huh7.5.1 cells. Culture media were collected from cells transfected with JFH1-EYFP, JFH1-EYFP mutant, JFH1-AsRed, or JFH1-AsRed mutant, respectively, and inoculated into uninfected Huh7.5.1 cells. EYFP- or AsRed-positive cells were

Figure 4 Localization and expression of NS5A-EYFP and NS5A-AsRed fusion proteins. (a,b) Huh7.5.1 cells transfected with JFH1-EYFP, AsRed and their mutant RNA genomes were fixed at 3 days post-transfection. NS5A-EYFP and NS5A-AsRed fusion proteins were visualized using EYFP and AsRed, respectively. DsRed auto-fluorescence was observed directly. NS5A and core proteins were immunostained with Alexa Fluor 488-labeled goat antimouse immunoglobulin G (green). 4′,6′-diamidino-2-phenylindole dihydrochloride (DAPI) (blue) staining revealed the nuclear chromatin. Bars represent 10 μm. (c) Cells were transfected with EGFP, JFH1, JFH1-EYFP, JFH1-AsRed, JFH1-EYFP mutant or JFH1-AsRed mutant. Cells were harvested at 3 days post-transfection, and western blotting was performed by using anti-GFP, NS5A or core antibodies.

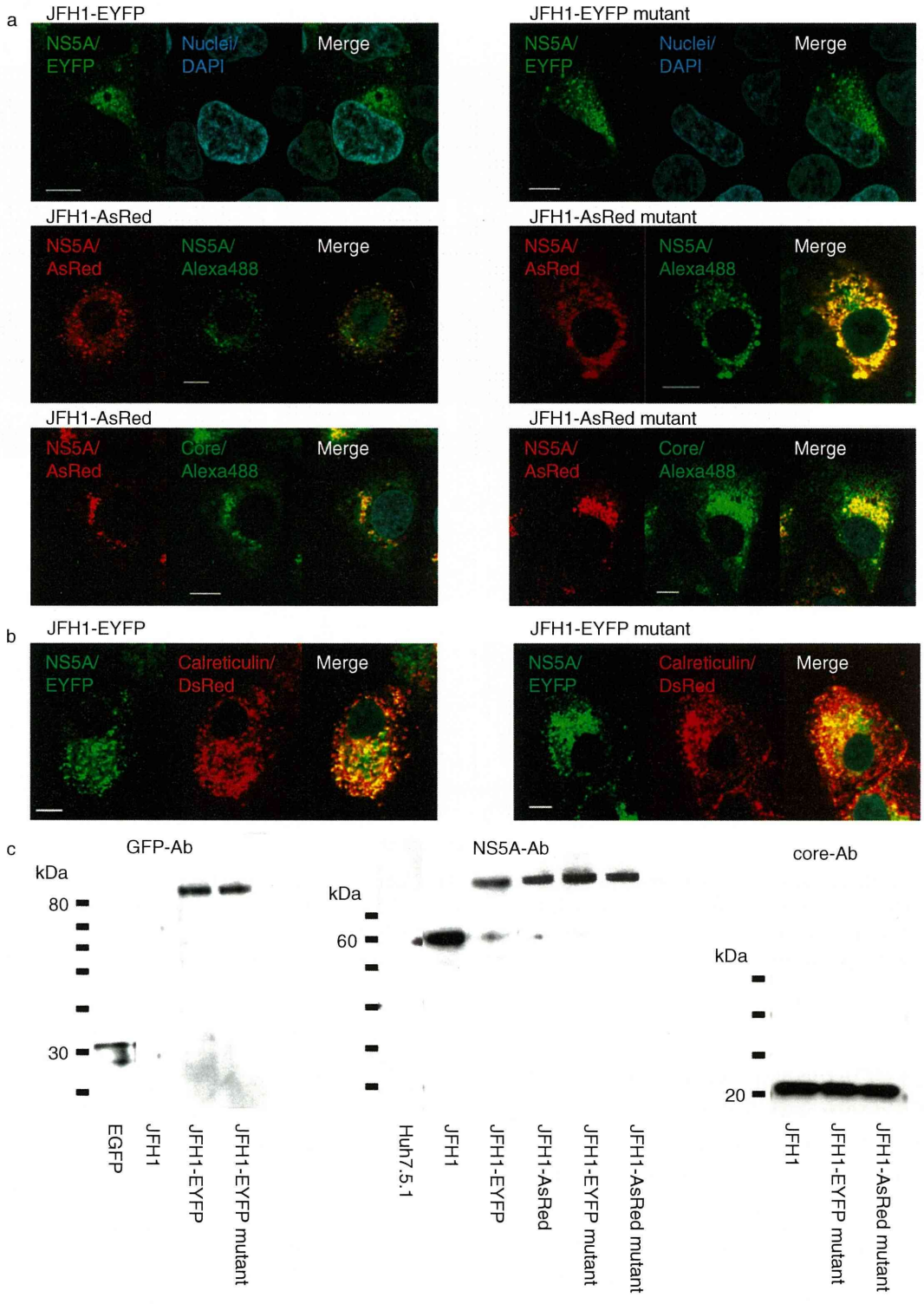

directly visualized by fluorescence microscopy on days 1–7. As shown in Figure 2(a), the number of cells positive for both JFH1-EYFP and JFH1-AsRed mutants, but not for JFH1-EYFP and JFH1-AsRed-infected cells, increased in a time-dependent manner. In JFH1-EFYP mutant-transfected cells, the proportion of EYFP-positive cells on days 3, 5 and 7 post-infection was 4.4%, 29% and 41%, respectively. In contrast, only 4.9% of JFH1-EYFP-transfected cells became EYFP-positive at 3 days post-infection, and the percentage of these fluorescence-positive cells decreased rapidly thereafter (Fig. 2b). Similarly, the percentage of cells infected with JFH1-AsRed mutant but not JFH1-AsRed increased exponentially. These results indicated that the two fluorescence virus clones with mutations are able to secrete infectious virus particles. We next compared levels of HCV core antigen in culture medium of cells infected with JFH1, JFH1-EYFP, JFH1-EYFP mutant, JFH1-AsRed, and JFH1-AsRed mutant viruses. The mutant viruses, but not the wild-type, produced amounts of core protein comparable to that of the parental JFH1 (Fig. 2C). In HCV-JFH1, JFH1-EYFP mutant, and JFH1-AsRed mutant-transfected cells, the core protein reached a peak of 1.25, 1.35 and 1.34 fmol/L, respectively, at 14 days post-transfection, while that of JFH1-EYFP JFH1-AsRed-transfected cells became undetectable at 10 days post-transfection. These results indicated that the mutant type is capable of producing an amount of viral particles comparable to that of the parental JFH1.

Using the two fluorescence-tagged viruses, we conducted co-infection of two virus strains, JFH1-AsRed mutant, which secreted infectious virus particles, and JFH1-EYFP, in which virus particle secretion was impaired. We collected culture media from cells transfected with JFH1-AsRed-mutant or JFH1-EYFP on day 2 post-transfection and infected both media onto uninfected Huh7.5.1 cells at a multiplicity of infection (moi, focus forming unit per cell) of 0.01. The number of JFH1-AsRed mutant-infected cells increased exponentially until day 3 but reached a plateau on days 5 and 7 post-infection. Interestingly, the number of cells positive for viral secretion-impaired JFH1-EYFP also increased in a manner similar to that of the JFH1-AsRed mutant (Fig. 3a). The percentage of AsRed mutant-positive cells was 4.6%, 6.7% and 14.8% at days 3, 5 and 7, respectively, while the percentage of EYFP-positive cells at the corresponding days was 3.1%, 4.8% and 5.1%, respectively (Fig. 3b). These results suggest that, in the co-culture of two HCV clones with and without virus particle secretion, a secretion-impaired virus clone is able to replicate and produce infectious particles possibly through the complementation of the intact virus.

Expression and subcellular localization of NS5A-fluorescence proteins

We next used fluorescence microscopy to study the subcellular localization of fluorescence and viral proteins. In cells transfected with JFH1-EYFP, JFH1-AsRed, and the respective mutants, EYFP and AsRed, were clearly visualized as dot-like structures in the perinuclear area (Fig. 4a). To determine if the NS5A-AsRed fusion protein indicates the subcellular localization of NS5A, we performed immunofluorescence staining of JFH-AsRed- and JFH1-AsRed mutant-infected cells using NS5A and HCV-core antibodies. Fluorescence of AsRed was co-localized precisely with NS5A and partially with core proteins. The fluorescence intensities of the JFH1-EYFP and -AsRed mutants within the cells were equal to that of the wild-type constructs. EYFP-NS5A of wild type and mutant JFH1 were localized in the ER (Fig. 4b). Western blotting was performed by using anti-GFP and anti-HCV-NS5A antibodies. As shown in Figure 4(c), three bands of the expected molecular weights of 27, 58 and 85 kDa, which corresponded to EGFP, NS5A and NS5A-EYFP fusion protein, were detected in EGFP, JFH1, JFH1-EYFP, JFH1-AsRed, JFH1-EYFP mutant, and JFH1-AsRed mutant-transfected cells. The expression levels of core protein in JFH1-EYFP mutant- and JFH1-AsRed mutant-transfected cells were almost the same as those transfected with parental JFH1. These results indicate

Figure 5 Kinetics of hepatitis C virus (HCV)-infected cells. (a) Huh7.5.1 cells were infected with JFH1-EYFP or JFH1-EYFP mutant HCV RNA. At the days indicated, cells were harvested and subjected to flow cytometry. EYFP-positive cells were sorted based on EYFP activating (*x*-axis) and staining with a marker of dead cells (*y*-axis). The results are depicted as density plots. The ratios of EYFP-positive cells vs time are shown below. Assays were carried out in triplicate and the results are expressed as mean ± standard deviation. $*P < 0.05$. $**P < 0.01$. —•—, JFH1-EYFP mutant; ··○··, JFH1-EYFP. (b) Culture media from JFH1-EYFP or mutant-transfected cells were added onto uninfected Huh7.5.1 cells at a moi of 0.01. At the days indicated, infected cells were analyzed using flow cytometry. The results are depicted as density plots. The ratio of EYFP-positive cells vs time are shown below. Assays were carried out in triplicate and the results are expressed as mean ± standard deviation. $*P < 0.05$. $**P < 0.01$. WT, wild type. —•—, JFH1-EYFP mutant; ··○··, JFH1-EYFP.

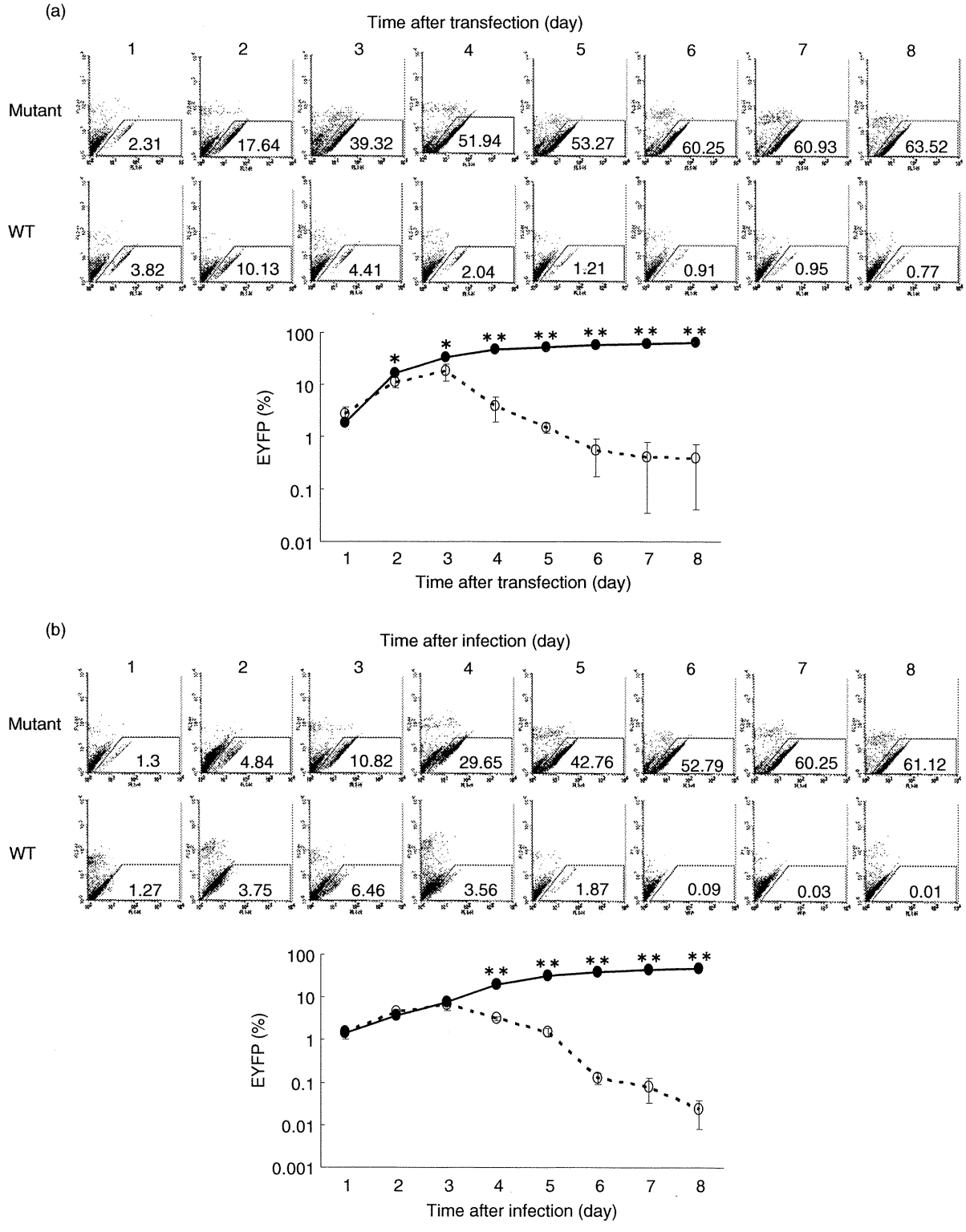

that the fusion proteins of NS5A and the fluorescent proteins remain intact within cells and serve as accurate markers of infection and as indicators of the subcellular localization of HCV-NS5A proteins.

Kinetics of HCV infection

Using those fluorescence-tagged HCV constructs, we analyzed more precisely the ratio and kinesics of HCV RNA-transfected cells and virus-infected cells by flow cytometry. After HCV RNA transfection, the percentages of JFH1-EYFP and JFH1-EYFP mutant-transfected cells were almost equivalent up to 2 days. Thereafter, JFH1-EYFP-positive cells began to decrease in number, while the mutant-transfected cells increased exponentially until 5 days post-transfection and then reached a plateau, when 52.2% of the cells were EYFP-positive (Fig. 5a). We collected the media from JFH1-EYFP and mutant-transfected cells at 2 days post-transfection, and added it onto uninfected Huh7.5.1 cells at a moi of 0.01. Similar to the results of the transfection assay, the population of JFH1-EYFP mutant-infected cells increased exponentially and reached a stable state at 6 days post-infection, when 39.2% of the cells were EYFP-positive (Fig. 5b). Calculating from the above data, the rate of expansion of HCV-infected cells was $2^{1.5}$/day. The cell-to-cell expansion of the JFH1-EYFP mutant infection was blocked by prior treatment of cells with anti-CD81 antibody (data not shown). This finding indicated that the expansion of the EGFP-positive cells was due to cell–cell spread of EYFP-tagged HCV and not the division of the virus-positive cells.

To further refine the calculation of the rate of cell-to-cell spread of infection, we carried out JFH1-EYFP mutant infection of uninfected Huh7.5.1 cells seeded at various densities from 2×10^3 to 2×10^5 cells/mL (Fig. 6). Flow cytometry showed that the rates of expansion of HCV-infected cells were $2^{1.5}$, $2^{2.3}$ and $2^{2.5}$/day at 2×10^3, 2×10^4 and 2×10^5 cells/cm^2, respectively. The ability of JFH1-EYFP to spread is greater in cells seeded at higher density. The maximum rate of expansion of HCV-infected cells was calculated as $2^{2.5}$/day.

Effects of antiviral drugs on HCV-infected cells

We next investigated the effects of antiviral agents on the infection kinetics of tagged-HCV. Eighteen hours after transfection of EYFP-tagged HCV RNA, the cells were treated with 10, 30 or 50 U/mL of IFN-α-2b or with 10 μM of protease inhibitor, BILN2061. JFH1-EYFP mutant-transfected cells were analyzed using flow cytometry. As shown in Figure 7, treatment of cells with the two compounds suppressed the time-dependent increase of HCV propagation. In addition, IFN-α-2b suppressed the dose-dependent increase of HCV

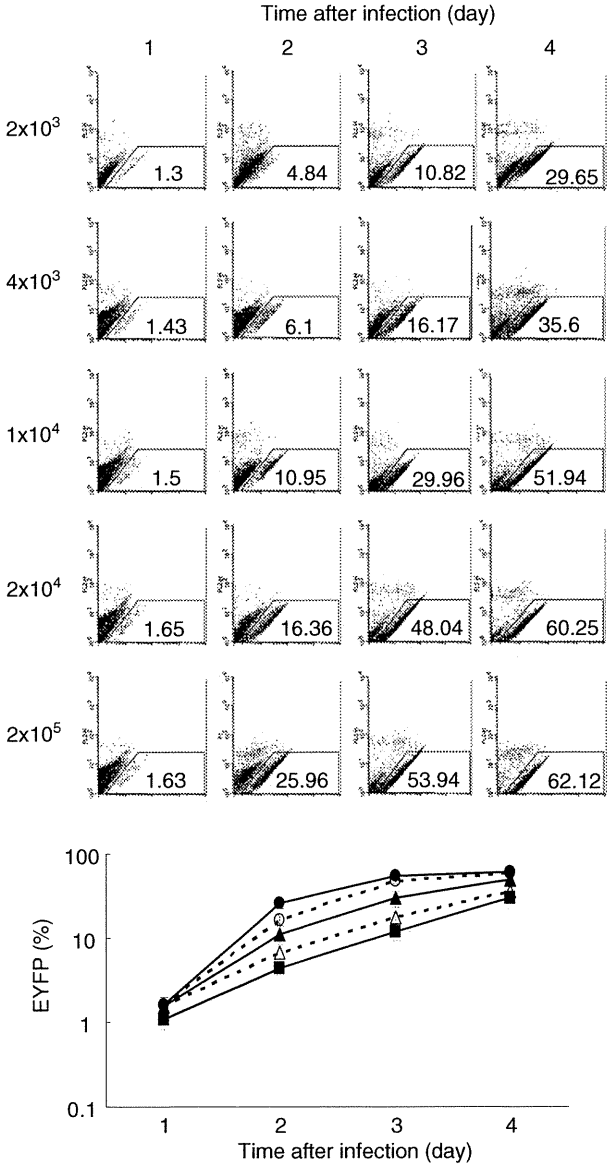

Figure 6 Rate of expansion of hepatitis C virus (HCV)-infected cells. The medium from JFH1-EYFP mutant was inoculated onto Huh7.5.1 cells seeded at different densities (2×10^3, 4×10^3, 1×10^4, 2×10^4 and 2×10^5 cells/cm^2) with core antigen adjusted doses. The results of flow cytometric analysis are depicted as density plots. The ratios of EYFP-positive cells vs time are shown beneath. Assays were carried out in triplicate and the results are expressed as mean ± standard deviation. —■—, 2×10^3; -·-, 4×10^3; —▲—, 1×10^4; -·-, 2×10^4; —●—, 2×10^5.

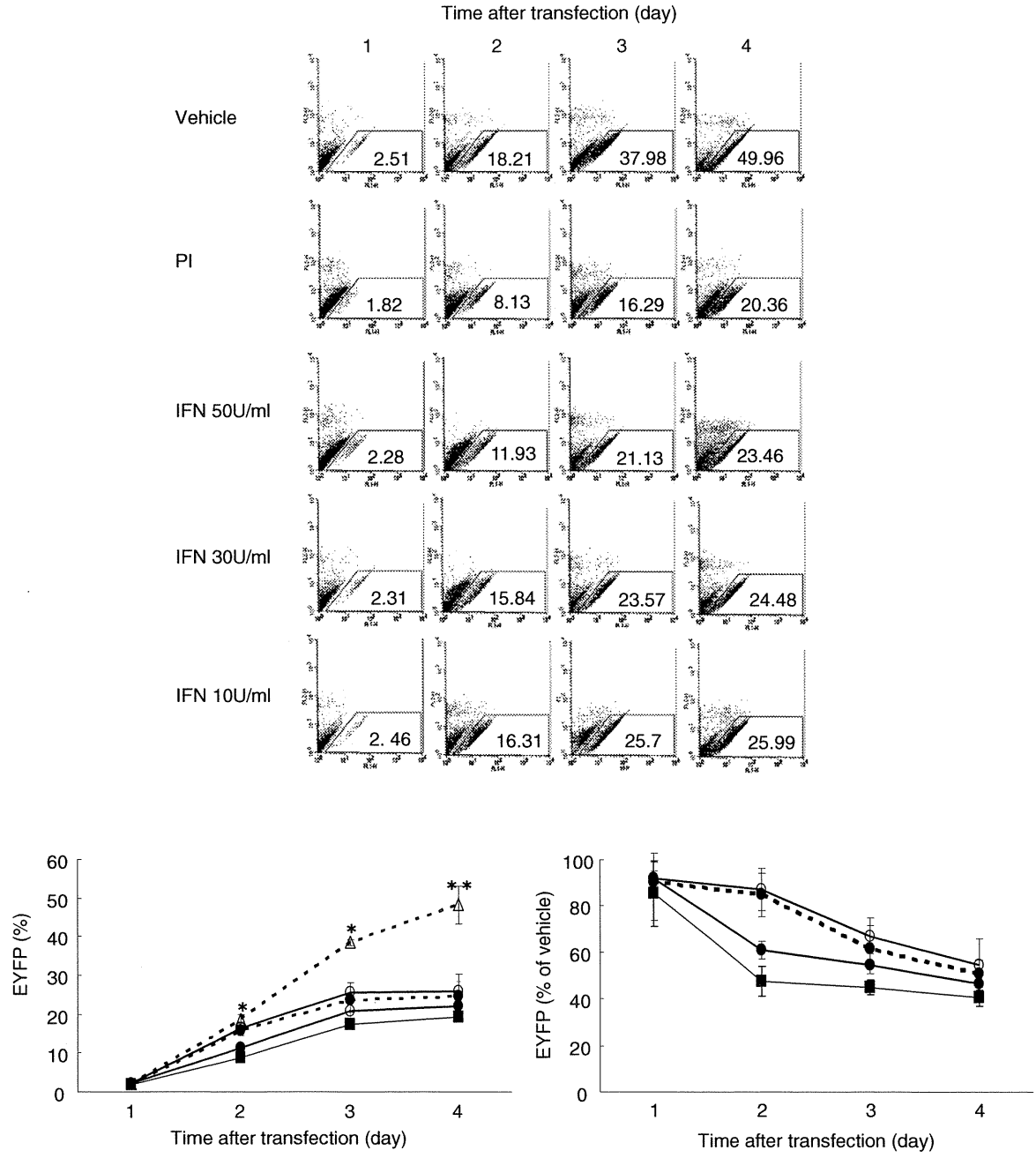

Figure 7 Effect of antiviral drugs on hepatitis C virus (HCV)-infected cells. Huh7.5.1 cells were transfected with JFH1-EYFP mutant RNA. Eighteen hours after transfection, cells were cultured with 10, 30 or 50 U/mL of interferon (IFN)-α-2b or 10 μM of the protease inhibitor BILN-2061. The cells were harvested at the days indicated and flow cytometry was performed. Ratios of EYFP-positive cells over time are shown at lower left. Plot values of 100% in each curve represent the EYFP expression levels in untreated cells (lower right). Assays were carried out in triplicate and the results are expressed as mean ± standard deviation. $^{*}P < 0.05$. $^{**}P < 0.01$. PI, protease inhibitor. -☆-, vehicle; —●—, 50 U/mL; -●-, 30 U/mL; —○—, 10 U/mL; —■—, PI.

propagation. At all time points, the number of infected cells was significantly lower in the culture treated with the two compounds than in the untreated culture. The protease inhibitor suppressed infection faster than did IFN-α-2b. These data indicate that IFN and the protease inhibitor were not only able to suppress intracellular HCV replication levels but also to inhibit virus particle secretion and expansion of HCV-infected cell populations.

DISCUSSION

IN THIS STUDY, we used fluorescence-tagged HCV, in which virus assembly, particle secretion and re-infection functions are fully preserved (Fig. 1).[17] Utilizing the fluorescence-tagged HCV, we analyzed the rate of expansion of HCV infection using live-cell flow cytometric analyses (Figs 5–7). In the early periods of infection, the expansion of the virus-positive cell population increased exponentially and the maximum rate of expansion was calculated as $2^{2.5}$/day. It is not clear why HCV propagation reaches a plateau, but this observation, where HCV replication is limited in confluent cells, has been made previously.[26] Possible explanations include cell death due to over-confluence, depletion of the nucleoside triphosphate pools in resting cells, and/or cell cycle-dependent effects on virus RNA replication and translation.

Co-infection of the two virus clones, EYFP-JFH1 and AsRed mutant JFH1, showed that viruses with impaired particle secretion were able to replicate and expand virus-infected cells (Fig. 3). Although we have found no clear mechanism to explain those effects, we speculate that the secretion-defective virus (JFH1-EYFP) may assemble into infectious virus through *trans*-complementation of virus proteins via co-infection in a single cell or recombination of mutant and wild-type virus genomic RNA. The co-infection experiment showed that the increase of JFH1-AsRed mutant-positive cells was slower than in the single clone infection experiment (Fig. 2a). These findings suggest that viruses with impaired particle secretion (JFH1-EYFP) partially suppressed expansion of viruses with intact particle secretion (JFH1-AsRed mutant) through *trans*-suppression of cellular virus replication or competitive binding to cellular virus entry receptors.

After the development of HCV-JFH1 cell culture,[11] many variations of HCV cell culture systems have been developed. Lindenbach *et al.* developed a genotype 2a intragenotypic chimera, J6/JFH, in which the JFH1 structural region was replaced with that of J6, isolated from a patient with chronic hepatitis.[27] The J6/JFH chimera is able to produce virus particles more efficiently than JFH1 but does not produce virus-induced cytopathic effects (CPE). Several marker protein-tagged viruses have been reported, in which viral infection could be visualized readily in living cells. A subgenomic replicon that expressed an NS5A-GFP fusion protein was reported first.[12] However, the clone lacked the structural regions that are required for virus propagation. Subsequently, full-length HCV reporter viruses were developed in which the EGFP gene was inserted into the NS5A-C-terminus of JFH1[13] or JC-1.[14] Jones *et al.* inserted the *renilla* luciferase gene into P7 of J6/JFH.[15] Unfortunately, the efficiency of virus production by the recombinant reporter viruses was greatly reduced compared to wild-type viruses. Very recently, it has been reported that a JFH1-based adaptive strain of a HCV reporter virus can produce infectious HCV particles as robustly as the JFH1 wild-type strain.[17] This virus system has overcome the serious limitations associated with the use and application of other reporter viruses.

Compared with the other HCV reporter viruses, the JFH1-EYFP/AsRed mutant is capable of producing amounts of HCV virus equivalent to that of the parental JFH1, which enables continuous passage of infection in cell culture and analyses using various research modalities, including flow cytometry and live-cell microcopy. Considering the current situation regarding the lack of singly effective, proven antiviral agents against HCV, other than IFN formulations, the search for potential antiviral agents will continue to be a dominant goal of research to improve clinical anti-HCV chemotherapeutics. This tagged HCV culture system may provide a very convenient tool for studies of the complete virus life cycle in live cells and of virus–host interactions, and it may be useful for high-throughput screening of drugs.

ACKNOWLEDGMENTS

WE THANK DR Frank Chisari for providing Huh7.5.1 cells and Boehringer Ingelheim for providing BILN2061. This study was supported by grants from the Ministry of Education, Culture, Sports, Science and Technology – Japan, the Japan Society for the Promotion of Science, Ministry of Health, Labor and Welfare – Japan, Japan Health Sciences Foundation, National Institute of Biomedical Innovation, and Miyakawa Memorial Research Foundation.

REFERENCES

1 Sangiovanni A, Prati GM, Fasani P *et al.* The natural history of compensated cirrhosis due to hepatitis C virus: a 17-year cohort study of 214 patients. *Hepatology* 2006; **43**: 1303–10.
2 Hiramatsu N, Oze T, Tsuda N *et al.* Should aged patients with chronic hepatitis C be treated with interferon and ribavirin combination therapy? *Hepatol Res* 2006; **35**: 185–9.
3 Fukuhara T, Takeishi K, Toshima T *et al.* Impact of amino acid substitutions in the core region of HCV on multistep hepatocarcinogenesis. *Hepatol Res* 2009; **40**: 171–8.
4 Tanaka Y, Nishida N, Sugiyama M, Tokunaga K, Mizokami M. lambda-Interferons and the single nucleotide polymorphisms: a milestone to tailor-made therapy for chronic hepatitis C. *Hepatol Res* 2010; **40**: 449–60.
5 Fried MW, Shiffman ML, Reddy KR *et al.* Peginterferon alfa-2a plus ribavirin for chronic hepatitis C virus infection. *N Engl J Med* 2002; **347**: 975–82.
6 Zeuzem S, Feinman SV, Rasenack J *et al.* Peginterferon alfa-2a in patients with chronic hepatitis C. *N Engl J Med* 2000; **343**: 1666–72.
7 Sakamoto N, Watanabe M. New therapeutic approaches to hepatitis C virus. *J Gastroenterol* 2009; **44**: 643–9.
8 Bartenschlager R, Lohmann V. Replication of hepatitis C virus. *J Gen Virol* 2000; **81**: 1631–48.
9 Mottola G, Cardinali G, Ceccacci A *et al.* Hepatitis C virus nonstructural proteins are localized in a modified endoplasmic reticulum of cells expressing viral subgenomic replicons. *Virology* 2002; **293**: 31–43.
10 Lohmann V, Koerner F, Koch J-O, Herian U, Theilmann L, Bartenschlager R. Replication of subgenomic hepatitis C virus RNAs in a hepatoma cell line. *Science* 1999; **285**: 110–3.
11 Wakita T, Pietschmann T, Kato T *et al.* Production of infectious hepatitis C virus in tissue culture from a cloned viral genome. *Nat Med* 2005; **11**: 791–6.
12 Moradpour D, Evans MJ, Gosert R *et al.* Insertion of green fluorescent protein into nonstructural protein 5A allows direct visualization of functional hepatitis C virus replication complexes. *J Virol* 2004; **78**: 7400–9.
13 Kim SS, Peng LF, Lin W *et al.* A cell-based, high-throughput screen for small molecule regulators of hepatitis C virus replication. *Gastroenterology* 2007; **132**: 311–20.
14 Schaller T, Appel N, Koutsoudakis G *et al.* Analysis of hepatitis C virus superinfection exclusion by using novel fluorochrome gene-tagged viral genomes. *J Virol* 2007; **81**: 4591–603.
15 Jones DM, Gretton SN, McLauchlan J, Targett-Adams P. Mobility analysis of an NS5A-GFP fusion protein in cells actively replicating hepatitis C virus subgenomic RNA. *J Gen Virol* 2007; **88**: 470–5.
16 Masaki T, Suzuki R, Murakami K *et al.* Interaction of hepatitis C virus nonstructural protein 5A with core protein is critical for the production of infectious virus particles. *J Virol* 2008; **82**: 7964–76.
17 Han Q, Xu C, Wu C, Zhu W, Yang R, Chen X. Compensatory mutations in NS3 and NS5A proteins enhance the virus production capability of hepatitis C reporter virus. *Virus Res* 2009; **145**: 63–73.
18 Lamarre D, Anderson PC, Bailey M *et al.* An NS3 protease inhibitor with antiviral effects in humans infected with hepatitis C virus. *Nature* 2003; **426**: 186–9.
19 Lin TI, Lenz O, Fanning G *et al.* In vitro activity and preclinical profile of TMC435350, a potent hepatitis C virus protease inhibitor. *Antimicrob Agents Chemother* 2009; **53**: 1377–85.
20 Zhong J, Gastaminza P, Cheng G *et al.* Robust hepatitis C virus infection in vitro. *Proc Natl Acad Sci USA* 2005; **102**: 9294–9.
21 Sekine-Osajima Y, Sakamoto N, Mishima K *et al.* Development of plaque assays for hepatitis C virus-JFH1 strain and isolation of mutants with enhanced cytopathogenicity and replication capacity. *Virology* 2008; **371**: 71–85.
22 Sekine-Osajima Y, Sakamoto N, Nakagawa M *et al.* Two flavonoids extracts from Glycyrrhizae radix inhibit in vitro hepatitis C virus replication. *Hepatol Res* 2009; **39**: 60–9.
23 Jin H, Yamashita A, Maekawa S *et al.* Griseofulvin, an oral antifungal agent, suppresses hepatitis C virus replication in vitro. *Hepatol Res* 2008; **38**: 909–18.
24 Itsui Y, Sakamoto N, Kakinuma S *et al.* Antiviral effects of the interferon-induced protein GBP-1 and its interaction with the hepatitis C virus NS5B protein. *J Gastroentorol* 2010; **45**: 523–36.
25 Nishimura-Sakurai Y, Sakamoto N, Mogushi K *et al.* Comparison of HCV-associated gene expression and cell signaling pathways in cells with or without HCV replicon and in replicon-cured cells1. *J Gastroenterol* 2009 (EPub ahead of print).
26 Iro M, Witteveldt J, Angus AG *et al.* A reporter cell line for rapid and sensitive evaluation of hepatitis C virus infectivity and replication. *Antiviral Res* 2009; **83**: 148–55.
27 Lindenbach BD, Meuleman P, Ploss A *et al.* Cell culture-grown hepatitis C virus is infectious in vivo and can be recultured in vitro. *Proc Natl Acad Sci USA* 2006; **103**: 3805–9.

Biochemical and Biophysical Research Communications 418 (2012) 313–318

Contents lists available at SciVerse ScienceDirect

Biochemical and Biophysical Research Communications

journal homepage: www.elsevier.com/locate/ybbrc

Identification of blood biomarkers of aging by transcript profiling of whole blood

Seiji Nakamura [a,*], Kozo Kawai [b], Yumie Takeshita [c], Masao Honda [c], Toshinari Takamura [c], Shuichi Kaneko [c], Ryo Matoba [a], Kenichi Matsubara [a]

[a] DNA Chip Research Inc., Suehiro-cho, Tsurumi-ku, Yokohama, Kanagawa 230-0045, Japan
[b] Department of Internal Medicine, Central Hospital of Matto-Ishikawa, Kuramitsu, Hakusan, Ishikawa 924-8588, Japan
[c] Department of Disease Control and Homeostasis, Kanazawa University Graduate School of Medical Science, Takara-machi, Kanazawa, Ishikawa 920-8641, Japan

ARTICLE INFO

Article history:
Received 16 December 2011
Available online 12 January 2012

Keywords:
Aging
Immune function
DNA microarray
Gene expression
Whole blood
Immune cells

ABSTRACT

Immunological changes that inevitably occur with aging are related to the onset of various diseases including autoimmune diseases, immunodeficiency, as well as other age-reflecting (AR) diseases. They are becoming serious problems in the global trend of longevity. To understand the AR changes, we searched for genes whose expression profiles in the whole peripheral blood change dramatically as a function of age using the Agilent whole human genome 44K microarray. After examining two cohorts consisting of 154 healthy people between age 23 and 77, we discovered 16 transcripts strongly and reproducibly correlated with age. Analysis using a publicly available gene expression dataset for a variety of human immune cells revealed that some of these transcripts were highly expressed in specific cell types whose number and function are known to change with age. This analysis shed light on the molecular mechanism of AR immunological system changes. Because of its simplicity, the assay system is expected to be useful for understanding individual health conditions.

1. Introduction

Senescent immune imbalance has been well known and is becoming a serious problem in the global trend of longevity. In addition to the typical disease-associated problems such as autoimmune diseases and immunodeficiency, the immune system of our body is steadily following paths of transition from the young to elderly. Causes, consequences, as well as mechanism of the immune system transition have been studied intensively, but these works have not reached systematic studies because of enormous variety of individuality [1–3].

One approach to this problem is to focus on age-reflecting (AR) shift of transcript balance in the peripheral blood mononuclear cells regardless of gender. Although factors that can affect the profile may be countless, such as those organ activities wherein immune cells are produced, nursed, educated, or mobilized to cope with changes of our physiological condition such as infection, damage of the body parts, hormone balance and drug-intake: These factors should be eliminated when we attempt to compare "normal" transcriptome profiles of man.

We undertook transcriptome studies with whole peripheral blood of normal, healthy people. Because isolation of peripheral blood mononuclear cells (PBMC) for analyses introduces technology-associated uncertainties, such as loss of significant fraction of white blood cells, loss of fragile transcriptome during the purification process, etc., we took whole peripheral blood as the starting material for this study.

Using simple correlation analyses, we compared blood from young, mature, and senior people for AR transcripts. We used two cohorts consisting of 154 healthy people, male and female, between age 23 through 77. Excluded were those regularly taking drugs, having been treated by doctors, or having biased biochemical data. We discovered 16 transcripts that behaved in AR fashion: Some were more abundant in older individuals (AR-increase), whereas others were less abundant in older individuals (AR-decrease). Here, we report results of the analyses, and describe some properties of these AR transcripts.

2. Materials and methods

2.1. Participants

Approval for the study was obtained from the Ethics Committee for Human Genome/Gene Analysis Research at Kanazawa University Graduate School of Medical Science. Blood samples were obtained from healthy volunteers at two related health examination sites in Ishikawa Prefecture: Hokkoku Clinic (site H), Public Central Hospital of Matto Ishikawa (site M). Of these volunteers, none needed routine doctor's visit nor were treated with any drugs. Informed consent was obtained from all subjects, and clinical data were collected.

* Corresponding author.
E-mail address: nakamura@dna-chip.co.jp (S. Nakamura).

0006-291X/$ - see front matter © 2012 Elsevier Inc. All rights reserved.
doi:10.1016/j.bbrc.2012.01.018

2.2. RNA extraction from blood

Blood samples were collected in PAXgene Blood RNA tubes (BD, NJ, USA), incubated and stored according to the manufacturer's protocol. Total RNA was extracted using the PAXgene Blood RNA Kit (QIAGEN, CA, USA) following the manufacturer's instructions. RNA quantity and quality were determined using a NanoDrop ND-1000 spectrophotometer (Thermo Scientific, DE, USA) and an Agilent 2100 Bioanalyzer (Agilent Technologies, CA, USA).

2.3. Microarray and data preprocessing

Cy3-labeled cRNA was synthesized from 250 ng of total RNA using Agilent Low RNA Input Linear Amplification Kit PLUS, One-Color (Agilent Technologies). After checking the quality and quantity of the cRNA using a NanoDrop ND-1000 spectrophotometer and an Agilent Bioanalyzer, the cRNA was hybridized at 65 °C for 17 hours to an Agilent Whole Human Genome Microarray 4 × 44K (Design ID: 014850). After washing, microarrays were scanned using an Agilent DNA microarray scanner (Agilent Technologies). All procedures from labeling to scanning were performed according to the manufacturer's instructions. Intensity values of each scanned feature were quantified using Agilent Feature Extraction Software, which performs background subtractions. Normalization was performed using Agilent GeneSpring GX version 11.0.2. (per chip normalization: 75 percentile shift; per gene normalization: none).

2.4. Extraction of the age-reflecting transcripts

Analysis was performed with probes annotated with Entrez Gene ID. Only those probes whose expression data were available at least 1 sample were taken for further analyses. Because the analyses were done on different occasions on samples from sites H and M, the batch cluster effect could give rise to bias to the microarray data. Therefore, we handled the data from the two sites independently to identify the AR transcripts. With this precaution, we selected transcripts whose expression levels correlated with age irrespectively of the two cohort sites. To further clarify the issue, Pearson's correlation and its significance between normalized gene expression levels and age were calculated under the R environment (http://cran.at.r-project.org), and transcripts with false discovery rate (FDR) of 0.25 or less in both sites were selected as the AR transcripts. We further confirmed the findings by taking GSE23515 in NCBI Gene Expression Omnibus (GEO) database [4] that included peripheral blood microarray datasets with age information.

2.5. Hierarchical clustering analysis

Hierarchical clustering analyses based on per gene normalization (divided by the median value of all samples for each transcripts) were performed by Spearman rank correlation similarity metric and complete linkage clustering algorithm using TIGR MultiExperiment Viewer software (http://www.tm4.org/). Distance threshold for dividing the cluster was set to 0.65.

2.6. Assignment of the AR transcripts to blood immune cell types

Identification of the source cells expressing the AR transcripts was done with GSE22886, the sets of Affymetrix microarray data from a variety of resting and activated human immune cells in NCBI GEO [4,5]. Probe information was combined with Entrez Gene ID. There were no Affymetrix probes corresponding to AMZ1 (Gene ID: 155185). Replicated data with the same cell type were averaged. Cell types that exceeded 1.5 IQR of the upper quartile were defined as "Expected cell types".

2.7. Real-time quantitative reverse transcription PCR

cDNA was synthesized from 500 ng total RNA using a High Capacity cDNA Reverse Transcription Kit (Applied Biosystems, CA, USA). Gene expression was analyzed by real-time quantitative PCR using Applied Biosystems 7900HT real-time PCR system. Specific sets of primers and TaqMan probes were obtained from Applied Biosystems. Gene expression level of the target transcript (CD248) was normalized with the values of an endogenous control gene (GAPDH).

Table 1
Summary of demographics of the subjects enrolled in this study.

	Site H	Site M
Subject number	90	64
Gender		
Male	46	35
Female	44	29
Age	40 ± 10 (min: 23, max: 66)	53 ± 11 (min: 27, max: 77)
BMI (kg/m^2)	21.1 ± 2.3 (min: 16.3, max: 27.5)	22.2 ± 2.7 (min: 16.6, max: 28.5)
sBP (mmHg)	110 ± 11 (min: 90, max: 144)	121 ± 16 (min: 92, max: 156)
dBP (mmHg)	66 ± 9 (min: 50, max: 90)	76 ± 9 (min: 57, max: 97)
AST (IU/L)	20 ± 5 (min: 10, max: 36)	21 ± 5 (min: 13, max: 30)
ALT (IU/L)	18 ± 8 (min: 6, max: 39)	19 ± 6 (min: 10, max: 32)
Glucose (mg/dL)	88 ± 9 (min: 76, max: 127)	94 ± 9 (min: 79, max: 120)
HbA1c (%)	5.0 ± 0.2 (min: 4.5, max: 5.6)	5.2 ± 0.3 (min: 4.2, max: 6.1)
Cholesterol (mg/dL)	188 ± 27 (min: 123, max: 245)	196 ± 29 (min: 134, max: 248)
HDL (mg/dL)	67 ± 14 (min: 40, max: 108)	62 ± 15 (min: 30, max: 94)
Triglycerides (mg/dL)	75 ± 33 (min: 30, max: 192)	89 ± 38 (min: 40, max: 194)
RBC (10^4/μL)	463 ± 46 (min: 345, max: 577)	463 ± 35 (min: 404, max: 569)
Platelet (10^4/μL)	22.8 ± 6.0 (min: 11.3, max: 38.0)	23.9 ± 5.8 (min: 10.6, max: 47.6)
WBC (/μL)	5688 ± 1388 (min: 2900, max: 9300)	4998 ± 1235 (min: 2910, max: 7940)
Neutrophil (/μL)	3455 ± 1095 (min: 1372, max: 6125)	2927 ± 940 (min: 1118, max: 5057)
Eosinophil (/μL)	147 ± 109 (min: 9, max: 539)	151 ± 104 (min: 12, max: 572)
Basophil (/μL)	35 ± 21 (min: 7, max: 112)	21 ± 12 (min: 0, max: 52)
Monocyte (/μL)	296 ± 104 (min: 129, max: 644)	261 ± 75 (min: 90, max: 449)
Lymphocyte (/μL)	1755 ± 505 (min: 896, max: 3572)	1638 ± 499 (min: 698, max: 3008)

Data are expressed as mean ± SD.